

**Rotating Disk-Electrode Aqueous Electrolyte Accelerated Stress Tests for PGM
Electrocatalyst/Support Durability Evaluation
DOE Durability Working Group
10/4/2011**

Conditions

Electrolyte: 0.1 to 1.0 M HClO₄ or 0.5 M H₂SO₄ (see Appendix A for discussion of effect of electrolyte)

Temperature: 25°C

Inert gas-purged electrolyte

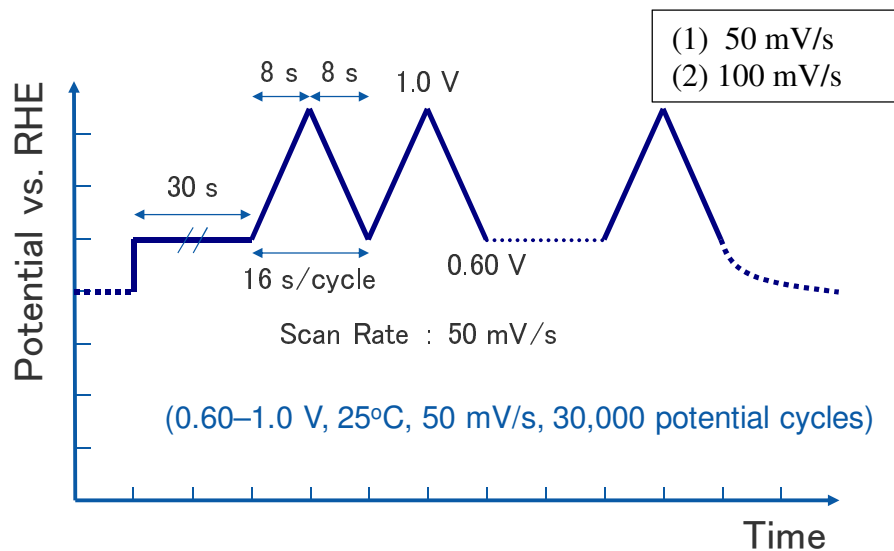
Stagnant solution during cycling

Proposed Protocols:

- (1) 0.6 to 1.0 V triangle wave at 50 mV/s (16 s/cycle; 133 h cycle time for 30,000 cycles) [Catalyst/support]
- (2) 0.6 to 1.0 V triangle wave at 100 mV/s (8 s/cycle; 67 h cycle time for 30,000 cycles) [Catalyst/support]
- (3) 0.4 to 1.05 V, square wave, 10 s/step (20 s/cycle; 167 h cycle time for 30,000 cycles) [Catalyst/support]
- (4) 1.0 to 1.6 V triangle wave at 100 mV/s (12 s/cycle; 100 h cycle time for 30,000 cycles) [Support]

Sources:

- (1) DOE Catalyst Durability Protocol for Sub-Scale MEAs
- (2) Variation of DOE Durability Protocol Proposed by S. Kocha to decrease cycle time
- (3) Square wave accelerated stress test proposed by M. Gummalla, UTRC, for sub-scale MEAs
- (4) Proposed protocol by S. Kocha for support durability



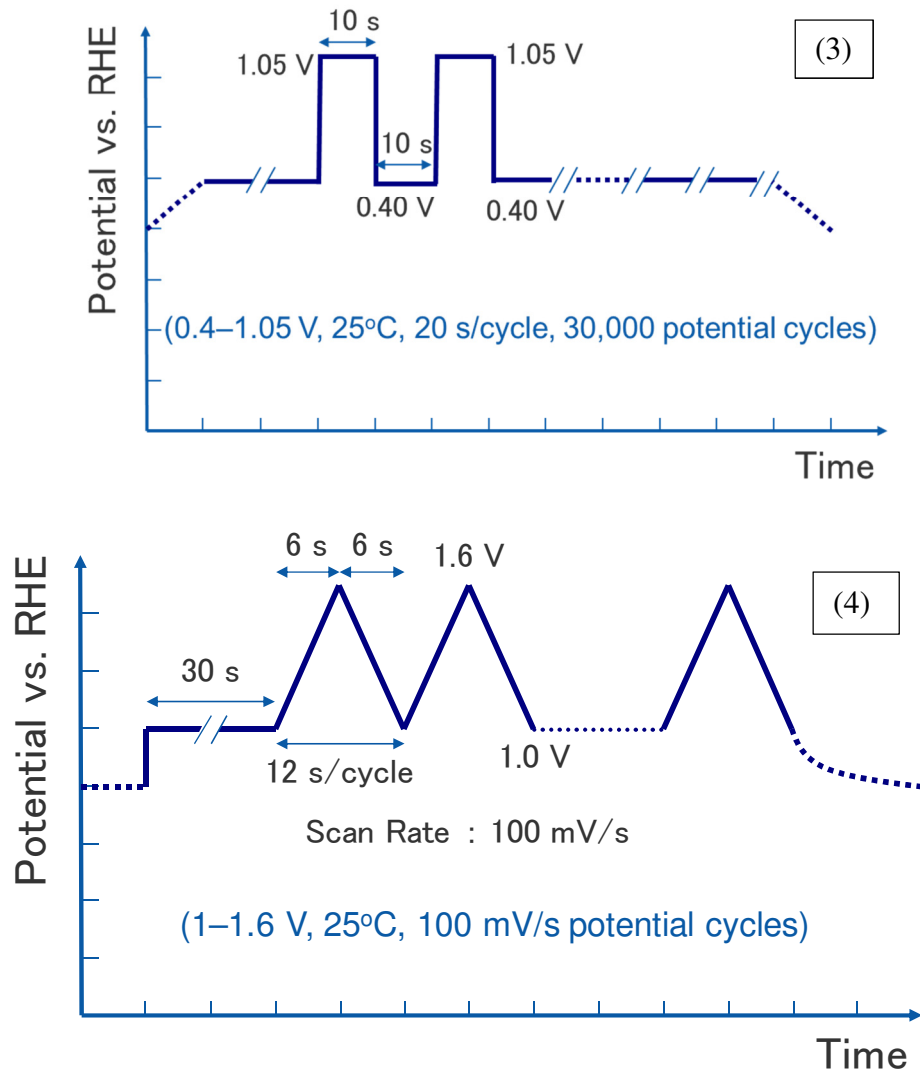


Fig. 1. Proposed ASTs profiles: (1) DOE protocol for catalysts in sub-scale MEAs, (2) Variation on DOE protocol to shorten cycle time, (3) Square wave cycle protocol for accelerated degradation rates, (4) Protocol for support degradation studies. Figures courtesy of Shyam Kocha, NREL.

Diagnostic measurements

The electrochemically-active surface area and oxygen reduction reaction activity of the catalyst should be determined, via the following recommended techniques, after 10, 100, 1k, 3k, 10k, 20k and 30k cycles.

1. Electrochemically-active surface area (ECA)

The electrochemically-active surface area (ECA) of the electrocatalyst should be determined via hydrogen adsorption/desorption and/or stripping of adsorbed CO.

Hydrogen adsorption/desorption:

Cyclic voltammograms between 0.05 and 0.4 V vs. RHE at 20 mV/s. No electrode rotation during measurement. Charges for hydrogen adsorption/desorption calculated by subtracting double layer and carbon capacitive background current, as shown in Fig. 1 (inset), and integrating charge in 0.05 to 0.4 V region. Alternatively, if CO is available, a more accurate background charge can be determined from a scan in the 0.05 to 0.4 V region in CO-saturated electrolyte, as shown in Fig. 2.¹

$$ECA(cm^2 Pt / gPt) = \frac{Q_H (\mu C / cm^2)}{210(\mu C / cm^2) Pt_{Loading} (gPt / cm^2)} \quad (1)$$

CO stripping:

Carbon monoxide (5N5 purity) purged through electrolyte while rotating electrode (e.g., 900 rpm) for 25 min. Electrode held at 0.05 V vs. RHE for 10 min. Electrolyte purged with inert gas for 25 min. while rotating electrode (e.g., 900 rpm). Rotation stopped. Voltammetric scan: 0.4 V to 0.05 V to 0.95 V to 0.05 V to 0.4 V at 20 mV/s. Charge for CO stripping charge calculated by integrating charge in 0.4 to 1.0 region in the anodic-going scan and subtracting background charge from 0.4 to 1.0 V in the first scan following the CO stripping scan (see Fig. 2).

$$ECA(cm^2 Pt / gPt) = \frac{Q_{CO} (\mu C / cm^2)}{420(\mu C / cm^2) Pt_{Loading} (gPt / cm^2)} \quad (2)$$

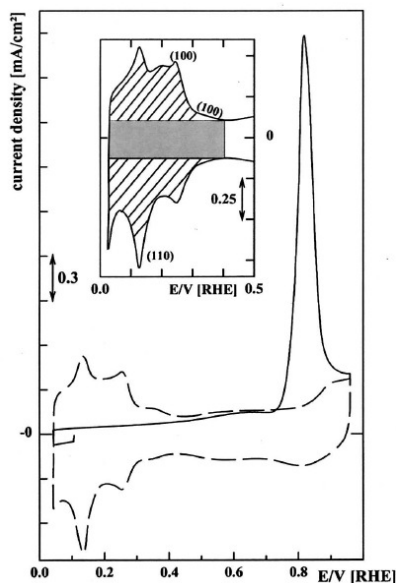


Fig. 2 Base voltammogram (---) and CO-stripping (—) from a Pt/Vulcan electrode on a rotating-disk electrode with a loading of $28 \mu g_{Pt}/cm^2$. (Inset) Grey rectangle - estimate of the charge contribution from Pt double-layer charging and the capacitance of the Vulcan support; the dashed pattern shows the hydrogen adsorption/desorption charge. Conditions: $25^\circ C$, 20 mV/s; 0.5 M H_2SO_4 . Reproduced from ².

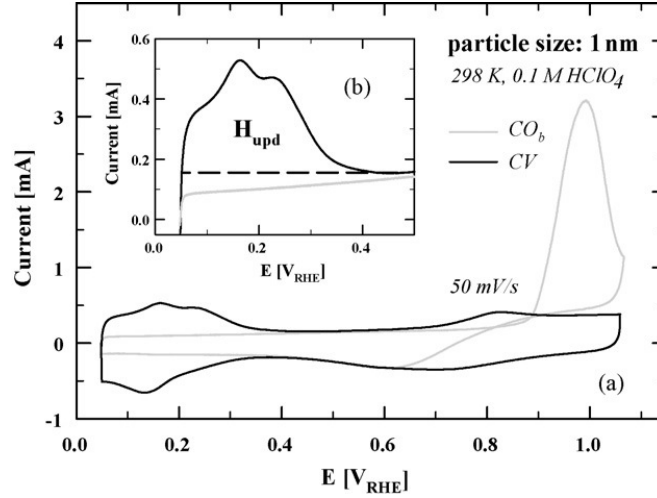


Fig. 3 Correction for the capacitive current caused by the carbon support using CO bulk oxidation (CO_b). CV in argon-purged solution (black) and the CO_b curve (grey)(a). The inset (b) demonstrates the conventional correction for capacity in the Hupd region (black dotted), the proper correction line from CO_b is shown in grey. In this case the ratio of Hupd:CO-stripping is 1.0:1.23 with conventional correction and 1.0:1.0 with the proper background correction. Reproduced with from ¹.

2. Oxygen reduction reaction activity

Electrolyte is saturated with oxygen (5N5 purity) by purging for at least 25 min. Multiple cyclic voltammograms are recorded between 0.05 V and 1.05 V at 20 mV/s while rotating electrode at 1600 rpm in O_2 -saturated electrolyte until a steady-state voltammogram is obtained. The pure ORR kinetic current can be extracted from the steady-state voltammograms using the mass transfer correction equation:^{1,3,4}

$$i_k = \frac{(i_{\text{lim}} \times i)}{(i_{\text{lim}} - i)} \quad (3)$$

where i is the measured current at a specified potential, i_{lim} is the measured limiting current, and i_k is the kinetic current. The assumptions for extracting i_k from the RDE data using Eq. (3) are valid over the current range of $0.1 i_{\text{lim}} < i < 0.8 i_{\text{lim}}$.¹ Area-specific activity and mass activity can be determined by calculation of i_k using Eq. 3 and normalization to measured catalyst ECA and catalyst loading, respectively. The ORR activity as extracted from the current at 0.9 V in the anodic-going voltammogram is reported (if current at 0.9 V is within validity range for Eq. (3)).

Notes: This technique provides activity that can be directly translated to the activity of the catalyst in an MEA as long as the weight of the catalyst is known precisely, the temperatures are comparable, the oxide coverages are similar, (i.e., the potential history immediately prior to the activity measurement is similar) and non-adsorbing electrolyte is used (e.g., perchloric acid electrolyte).^{3,5,6} (see Appendix B for a discussion of catalyst film requirements for the RDE and RRDE techniques).^{3,4}

Parameters to be reported for diagnostic measurements:

Method used, electrolyte type and concentration, scan rate, scan direction for ORR measurement, reference electrode used and method for converting to RHE scale, temperature, and constant used for calculating ECA.

References

- 1 Mayrhofer, K. J. J. *et al.* Measurement of oxygen reduction activities via the rotating disc electrode method: From Pt model surfaces to carbon-supported high surface area catalysts. *Electrochim Acta* **53**, 3181-3188 (2008).
- 2 Schmidt, T. J. *et al.* Characterization of high-surface area electrocatalysts using a rotating disk electrode configuration. *J Electrochem Soc* **145**, 2354-2358 (1998).
- 3 Gasteiger, H. A., Kocha, S. S., Sompalli, B. & Wagner, F. T. Activity benchmarks and requirements for Pt, Pt-alloy, and non-Pt oxygen reduction catalysts for PEMFCs. *Appl Catal B-Environ* **56**, 9-35 (2005).
- 4 Paulus, U. A., Schmidt, T. J., Gasteiger, H. A. & Behm, R. J. Oxygen reduction on a high-surface area Pt/Vulcan carbon catalyst: A thin-film rotating ring-disk electrode study. *J Electroanal Chem* **495**, 134-145 (2001).
- 5 Schmidt, T. J. & Gasteiger, H. A. in *Handbook of Fuel Cells: Fundamentals Technology and Applications* Vol. 3 (eds W. Vielstich, H.A. Gasteiger, & A. Lamm) 316 (Wiley, 2003).
- 6 Takahashi, I. & Kocha, S. S. Examination of the activity and durability of PEMFC catalysts in liquid electrolytes. *J Power Sources* **195**, 6312-6322 (2010).
- 7 Ramani, V. K. in *Department of Energy Hydrogen Program 2011 Annual Merit Review* (Arlington, VA, 2011).
- 8 Ball, S. C., Hudson, S., Theobald, B. & Thompsett, D. Enhanced stability of PtCo catalysts for PEMFC. *Electrochemical Society Transactions* **1**, 141-152 (2006).
- 9 Myers, D. J. *et al.* in *2011 U.S. DOE Hydrogen and Fuel Cells Program Annual Merit Review and Peer Evaluation Meeting* FC012 (Arlington, VA, 2011).
- 10 Holby, E. F., Sheng, W. C., Shao-Horn, Y. & Morgan, D. Pt nanoparticle stability in PEM fuel cells: Influence of particle size distribution and crossover hydrogen. *Energ Environ Sci* **2**, 865-871 (2009).
- 11 Nagai, T., Murata, H. & Morimoto, Y. The Influence of Experimental Conditions on the Catalyst Degradation in the Accelerated Durability Test using a Rotating Disk Electrode. *Electrochemical Society Transactions* **To be published.** (2012).
- 12 Garsany, Y., Baturina, O. A., Swider-Lyons, K. E. & Kocha, S. S. Experimental methods for quantifying the activity of platinum electrocatalysts for the oxygen reduction reaction. *Anal Chem* **82**, 6321-6328 (2010).
- 13 Mansfeld, F. B. & Kenkel, J. V. Contamination of test electrolytes by dissolution products of platinum counter electrodes. *Corrosion* **31**, 149-150 (1975).
- 14 Bard, A. J. & Faulkner, L. R. *Electrochemical methods: Fundamentals and applications.* (John Wiley & Sons, 1980).

- 15 Pletcher, D. *A first course in electrode processes* Edition: 2nd edn, (Cambridge: Royal Society of Chemistry, 2009).
- 16 Gloaguen, F., Convert, P., Gamburzev, S., Velev, O. A. & Srinivasan, S. An evaluation of the macro-homogeneous and agglomerate model for oxygen reduction in PEMFCs. *Electrochim Acta* **43**, 3767-3772 (1998).
- 17 Perez, J., Gonzalez, E. R. & Ticianelli, E. A. Impedance studies of the oxygen reduction on thin porous coating rotating platinum electrodes. *J Electrochem Soc* **145**, 2307-2313 (1998).
- 18 Higuchi, E., Uchida, H. & Watanabe, M. Effect of loading level in platinum-dispersed carbon black electrocatalysts on oxygen reduction activity evaluated by rotating disk electrode. *J Electroanal Chem* **583**, 69-76 (2005).
- 19 Wang, C. *et al.* Multimetallic Au/FePt₃ nanoparticles as highly durable electrocatalyst. *Nano Lett* **11**, 919-926 (2011).
- 20 Sheng, W. C., Gasteiger, H. A. & Shao-Horn, Y. Hydrogen oxidation and evolution reaction kinetics on platinum: Acid vs alkaline electrolytes. *J Electrochem Soc* **157**, B1529-B1536 (2010).
- 21 Lawson, D. R., Whiteley, L. D., Martin, C. R., Szentirmay, M. N. & Song, J. I. Oxygen reduction at Nafion film-coated platinum electrodes - Transport and kinetics. *J Electrochem Soc* **135**, 2247-2253 (1988).

Appendix A. Discussion on effect of type of electrolyte

Previous literature has shown varying degrees of correlation between catalyst degradation rates in aqueous and MEA environments.[12,19] For example, recent data from Nissan Technical Center of North America showed excellent correlation between loss of electrochemically-active surface area (ECA) of Pt nanoparticles supported on high surface area carbon when cycled between 1.0 and 1.5 V for 1,000 cycles in a large volume rotating disk-electrode (RDE) cell with 0.1 M HClO₄ electrolyte versus in a fuel cell environment.⁷ Ball et al., however, found a greater loss of ECA for a carbon-supported Pt nanoparticle catalyst in a 1 M H₂SO₄ aqueous electrolyte versus the fuel cell environment over 10,000 cycles between 0.6 and 1.0 V (75% versus 52%).⁸ Myers et al. found a lower loss of ECA for Pt/C in a small volume room temperature aqueous 0.1 M HClO₄ as compared to the fuel cell environment at 80°C in square and triangle cycles between 0.4 and 1.05 V and 0.6 and 1.0 V, respectively.⁹ Comparing electrolytes, Takahashi and Kocha found that ECA losses were higher in sulfuric acid electrolyte versus perchloric acid electrolyte, as shown in Fig. 1.2. They suggested that sulfuric acid electrolyte is a more suitable electrolyte than perchloric acid for simulated fuel cell durability tests for Pt-based electrocatalysts due to the similar onset potentials for oxide formation in the fuel cell environment and sulfuric acid electrolyte.⁶ Takahashi and Kocha also found that ECA losses for Pt/C and Pt₃Co/C due to potential cycling in sulfuric acid electrolyte were in qualitative agreement with ECA losses reported for fuel cells.⁶

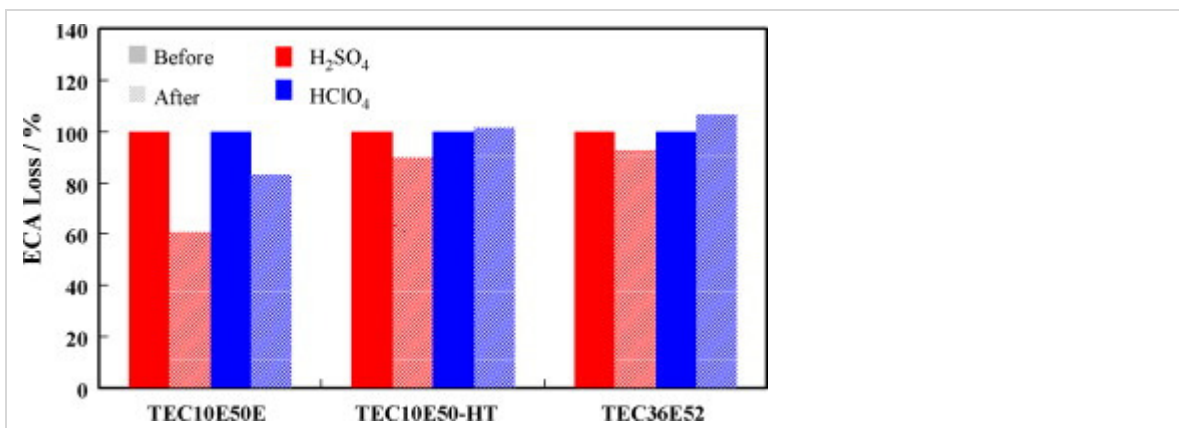


Fig. 1.2 Comparison of the loss in ECA after potential cycling in aqueous 25°C sulfuric acid or perchloric acid electrolyte for Tanaka's Pt/C (TEC10E50E), heat-treated Pt/C (TEC10E50-HT), and PtCo/C (TEC36E52) catalysts. Potential cycling protocol: 7200 square wave cycles between 0.6 to 1.0 V vs. the reversible hydrogen electrode (RHE), 2 s/cycle. Reprinted with permission from ⁶.

Modeling work by Holby et al.¹⁰ suggested that the presence of a “sink” for dissolved platinum is an important factor controlling extent of ECA loss and changes in Pt particle size distribution. In the fuel cell environment, hydrogen crossing through the membrane from the anode reduces dissolved Pt to metallic Pt in the membrane. The presence of this

“sink” for dissolved Pt accelerates Pt dissolution and loss of Pt mass from the electrode compared to equivalent cycles without crossover hydrogen, such as in a liquid electrolyte.¹⁰ However, comparison of loss of ECA and changes in Pt particle size distribution in aqueous electrolyte half-cell measurements must also take into account the ratio of initial ECA to electrolyte volume as this ratio controls the evolution of the concentration of dissolved Pt with time and thus the extent of Pt loss from the electrode and the kinetics of Pt re-deposition.¹⁰ These measurements must also take into account the transport of dissolved Pt away from the electrode surface (e.g., by rotation of the electrode in a rotating-disk electrode). For example, Nagai et al. recently reported that the loss of ECA of Pt nanoparticles on an RDE increased with increasing the rotation rate and/or decreasing the catalyst amount.¹¹ These two important aspects may be the cause of the disparate ECA loss results in aqueous electrolyte studies of electrocatalyst stability mentioned previously.

The utility of aqueous tests for long-term durability tests may be limited due to the adsorption of electrolyte impurities on the electrocatalyst surface, which may lead to apparent loss of ECA and electrocatalytic activity. These impurities may arise from the acids or water used to make the dilute electrolytes, from the electrochemical cell (e.g., the glassware), or from the counter or reference electrodes.^{6,12} The judicious choice of counter and reference electrodes, the reference electrode filling solution, and isolation of these electrodes from the electrocatalyst working electrode via frits, Luggin capillaries, or membranes can minimize or eliminate these sources of impurities. It should be mentioned that adsorption of impurities on the electrocatalyst can be the source of not only decreases in apparent electrocatalytic activity, but also increases, such as those that may arise from dissolution of a platinum counter electrode and deposition of the dissolved platinum on an electrocatalyst with lower intrinsic electrocatalytic activity than platinum.¹³ Three-electrode aqueous cell design and proper isolation and placement of counter and reference electrode have been discussed in numerous manuscripts and electrochemical textbooks.^{14,15} In addition, adherence of the catalyst film to the underlying electrically conductive substrate (e.g., glassy carbon electrode), can limit the duration of degradation tests in aqueous electrolyte especially under hydrodynamic conditions.⁶

Appendix B. Requirements for accurate ORR kinetics using RDE method

The accurate evaluation of the kinetics of PEFC-relevant reactions using hydrodynamic techniques requires formation of a thin film of the electrocatalyst material to eliminate the effects of diffusion within the film and utilization of the materials. As described by Mayrhofer et al., there are three main requirements that must be fulfilled for thin film hydrodynamic techniques, such as thin film-rotating disk electrode (TF-RDE), to provide reliable kinetic data: (1) The theoretical diffusion limited current density must be achieved, (2) the catalytic activity normalized to catalyst weight or surface area must be independent of the loading of catalyst on the working electrode (i.e., the disk in the RDE or RRDE techniques), and (3) the catalytic activity should be calculated at currents approximately half that of the diffusion limited current.¹ Attaining these three criteria

requires careful deposition of the catalyst on the disk to achieve uniform and complete coverage and adjustment of the loading of catalyst while maintaining this coverage.^{6,12} The thin film must also be <0.1 μm thickness to eliminate effects of mass transfer within the film, non-ideal transport of reactants to the disk electrode and intermediates to the downstream electrode (i.e., the ring electrode in RRDE), and poor electronic contact within the film.¹⁶⁻¹⁸ There are three common techniques for forming thin films of catalyst powders on the substrates used for hydrodynamic techniques, such as the glassy carbon disk electrodes of RDE or RRDEs: (1) deposition of a composite of the catalyst powder and perfluorosulfonic acid polymer,³ (2) deposition of catalyst powder from a suspension of the powder in water and/or alcohol followed by deposition of a thin film of perfluorosulfonic acid ionomer,^{1,2,4} or (3) deposition of the catalyst powder from a water suspension without the use of a binder.^{19,20}

A rigorous analysis of the validity of the assumption of lack of mass transport effects within the thin film involves analysis of the rotation rate dependence of the current. Equation (3) can be expanded to take into account the effects of diffusion within a film electrode:²¹

$$\frac{1}{i} = \frac{1}{i_k} + \frac{1}{i_f} + \frac{1}{i_{lim}} = \frac{1}{i_k} + \frac{1}{i_f} + \frac{1}{K\omega^2} \quad (4)$$

where i_f represents the film-diffusion-limited current or current density controlled by reactant diffusion within the electrode film, K is a constant dependent on oxygen concentration, the diffusion coefficient of oxygen in the electrolyte, and on its kinematic viscosity, ω is the angular rotation velocity of the RDE, and the other terms have the same meaning as in Eqn. (3). A Koutecky-Levich plot, $1/i$ vs. $1/\omega^{1/2}$, for a fixed potential should show a linear relationship with a slope of $1/K$ and a y-intercept of $1/i_k + 1/i_f$.¹⁴ To determine if film diffusion is affecting the kinetic currents obtained from RDE measurements and to correct for its effect, the y-intercept of the Koutecky-Levich plot for $i=i_{lim}$ is subtracted from the y-intercept for the same plot at the potential of interest. Comparison of the kinetic currents derived directly from the y-intercepts of the Koutecky-Levich plots (i_k) to those corrected for film diffusion indicates the extent of the influence of film diffusion on the RDE measurements.

Excellent discussions of the use of RDE for ORR activity measurements can be found in Mayrhofer et al.,¹ Garsany et al.,¹² Takahashi et al.,⁶ and Schmidt and Gasteiger.⁵